Isolated attosecond pulses generated from a relativistic plasma mirror via noncollinear gating

Hyeon Kim,[1,2] Chul Min Kim,[1,3] Ki Hong Pae,[1,3] and Kyung Taec Kim[1,2,*]
[1]*Center for Relativistic Laser Science, Institute for Basic Science, Gwangju 61005, Republic of Korea*
[2]*Department of Physics and Photon Science, Gwangju Institute of Science and Technology, Gwangju 61005, Republic of Korea*
[3]*Advanced Photonics Research Institute, Gwangju Institute of Science and Technology, Gwangju 61005, Republic of Korea*

(Received 2 September 2024; accepted 11 February 2025; published 27 February 2025)

A train of intense attosecond pulses can be obtained through relativistic high harmonic generation when an intense laser field is reflected on a plasma surface. Separating a single isolated attosecond pulse from the train is critical not only for applications such as time-resolved pump-probe experiments but also for studying laser-plasma interactions with attosecond temporal resolution. Various methods have been developed for an isolated attosecond pulse generation in gas. However, they require ultrashort laser pulses, which are difficult to apply with high-power lasers typically employed in relativistic high harmonic generation. Here, we demonstrate that an isolated attosecond pulse can be obtained through relativistic high harmonic generation using noncollinear temporal gating. Our approach also provides direct access to each attosecond pulse in the train, allowing us to diagnose the laser-plasma interaction, such as plasma denting and reflection positions, in a time-resolved manner. Thus, it offers breakthroughs in attosecond pulse generation at relativistic laser intensities.

DOI: 10.1103/PhysRevResearch.7.013216

I. INTRODUCTION

When an intense laser beam irradiates a medium, a plasma is instantly created on the surface of the medium. If the plasma density is high enough, the incident laser beam can be fully reflected [1,2]. This phenomenon is called a plasma mirror [1,2]. When the intense laser field is reflected, charged particles in the plasma can be driven by the laser field to relativistic speed. This highly nonlinear motion of the electrons yields attosecond pulses [3–7]. Since this process is repeated in the oscillating laser field, a train of attosecond pulses is generated which forms a high harmonic spectrum in the frequency domain.

Due to their superb temporal and spatial coherent properties, attosecond pulses obtained through relativistic high harmonic generation (HHG) from a plasma mirror have gained significant attention for decades [4–7]. They hold great potential for applications such as pump-probe experiments and coherent diffraction imaging [8]. For these applications, it is desirable to isolate a single attosecond pulse from the train. In the case of high harmonic generation in gas, several methods have been successfully demonstrated for the generation of isolated attosecond pulses, including amplitude gating [9–11], ionization gating [12,13], polarization gating [14,15], the attosecond lighthouse effect [16–18], and noncollinear optical gating [19]. These developments have made a great advancement in strong field physics and attosecond science [20].

In the context of plasma-based high harmonic generation, research has also been conducted for generating isolated attosecond pulses. Similar to gas harmonics, methods such as few-cycle driving [21], temporal gating like polarization gating [22], spatiotemporal noncollinear optical gating [23], the attosecond lighthouse effect [16,18], and a mixed scheme of polarization and noncollinear gating [24] have been suggested. Also, a new approach called cascade method that utilizes the response of the plasma is also suggested for the generation of isolated attosecond pulses [25]. Some of them showed experimentally the capability to generate isolated attosecond pulses [18,24].

Although many approaches have been successfully suggested, all the techniques essentially require an ultrashort driving laser pulse. Such an ultrashort laser pulse is obtained using pulse compression techniques [25]. The achievable peak power for near-single-cycle or few-cycle pulses with available technology is ∼1 TW [26], corresponding to an intensity of $\sim 10^{19}\ \mathrm{W/cm^2}$ when the laser beam is tightly focused. Due to this limitation, the experimental demonstrations of the aforementioned gating techniques were performed using low-power lasers only [18,24].

To address these issues, we present an approach for the generation of isolated attosecond pulses through relativistic high harmonic generation. Our method focuses on angularly separating a single, isolated attosecond pulse from the attosecond pulse train in the far field. We use two laser pulses which are superposed in a small angle at the plasma surface. One pulse is an intense and long main pulse. The other laser pulse is a significantly weak and single-cycle laser pulse. This combination of laser pulses with different incidence angles allows for the effective isolation of attosecond pulses. Through

*Contact author: kyungtaec@gist.ac.kr

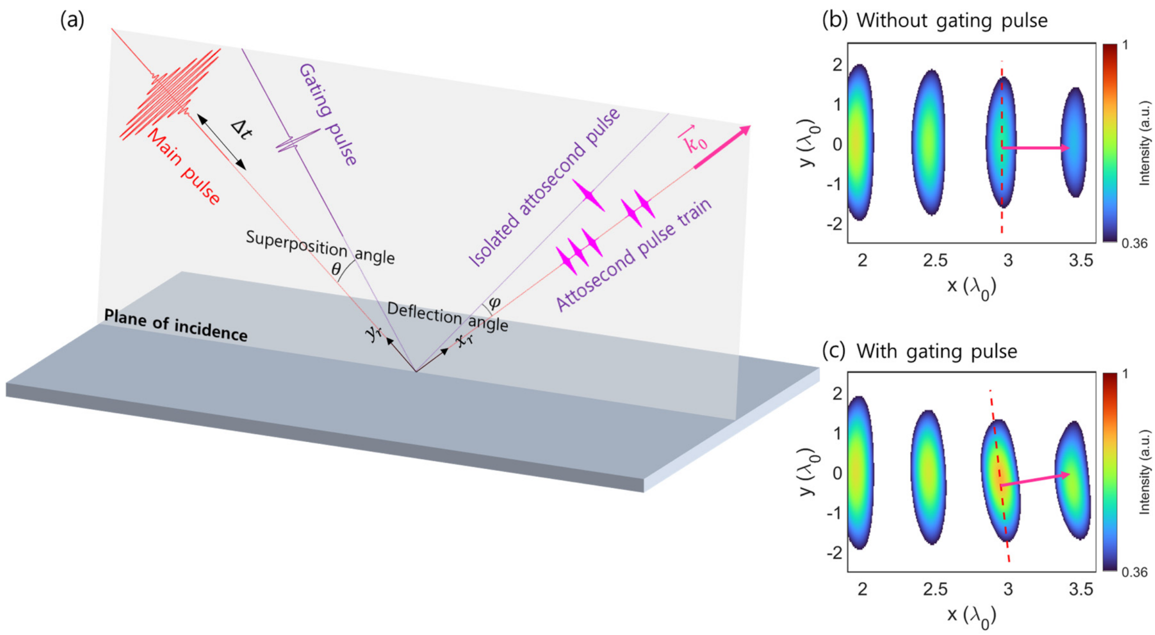

FIG. 1. Schematic illustration of separation of an isolated attosecond pulse. (a) Generation of attosecond pulse train and separation of an isolated attosecond pulse. The main pulse is intense and long. The gating pulse is relatively weak and short. The two pulses are incident on the plasma surface at a relative angle θ and with a delay Δt. (b) The electric field of the main pulse. (c) The electric field obtained by superposing the two beams with $\theta = 170$ mrad and $\Delta t = -3T_0$.

extensive numerical simulations and analysis, we demonstrate the efficacy of our approach. We show that an isolated attosecond pulse can be successfully separated using a long driving laser pulse with an intensity of 1×10^{21} W/cm^2 by superposing a short gating pulse with an intensity of 1.9×10^{19} W/cm^2.

The separation of the isolated attosecond pulse also allows us to directly access the temporal profile of the attosecond pulse train. By changing the time delay between the two laser pulses, we could observe the attosecond pulse train that contains information on the laser-plasma interaction. We found that the temporal separations of the attosecond pulses are varying in time, manifesting the plasma denting effect. We could reconstruct the reflection point where the attosecond pulses are generated, which is critical to understand the mechanism of relativistic high harmonic generation [27]. Consequently, our approach not only provides a practical method for generating isolated attosecond pulses but also for investigating the laser-plasma interaction with subcycle attosecond temporal resolution.

II. RESULTS AND DISCUSSION

When an intense laser field is obliquely incident on a dense plasma, the laser field is reflected on the surface of the plasma as shown in Fig. 1. The charged particles, both electrons and ions in the plasma, are accelerated while the laser field is reflected. If the laser field is intense enough ($a_0 > 1$), the speed of the electrons, which are lighter, can reach relativistic speeds. Here, a_0 is a normalized vector potential. The electron motion becomes highly nonlinear, radiating a high-frequency emission within a subcycle duration. These attosecond pulses are emitted repeatedly at every optical cycle of the laser field from the electrons distributed in the laser beam. Since the intensity and phase (or wave front) of the driving laser beam are symmetric along the beam axis, the generated attosecond pulse propagates along the propagation direction $\boldsymbol{k}_0$ of the reflected laser beam, as shown in Fig. 1.

The propagation direction of the attosecond pulses is determined by the amplitude and phase of the driving laser beam within the interaction volume. Thus, the propagation direction can be controlled by changing the wave front of the driving laser field. One way to implement such a manipulation is to impose a wave-front rotation by imposing an angular dispersion on the driving laser beam [16,18]. However, it is difficult to apply this approach to ultrahigh intensity laser beams because it requires a broadband laser beam.

To manipulate the wave front of the driving laser beam, we use an additional laser beam whose intensity is much weaker than that of the driving laser field. When these two beams are superposed, the wave front of the laser beam can be manipulated depending on the superposition angle θ and the time delay Δt between the two pulses as shown in Fig. 1. When the additional laser field is added, the wave-front rotation is clearly observed as shown in Figs. 1(b) and 1(c). Thus, the attosecond pulse generated at this single optical cycle can be deflected.

The wave-front rotation can be expressed with the deflection angle $\varphi(t)$ induced by the superposition of the two laser pulses. Provided that both of the laser pulses have a Gaussian envelope, $\epsilon_1 = E_1 \exp[-2\ \ln(2)(t)^2/\tau_1^2]$ and $\epsilon_2 = E_2 \exp[-2\ \ln(2)(t-\Delta t)^2/\tau_2^2]$. Here, E and τ denote the field amplitude and duration. The deflection angle $\varphi(t)$ for a small superposition angle θ can be expressed as

$$\varphi(t) = \frac{\theta \xi(t)}{1 + \xi(t)}, \tag{1}$$

where $\xi(t)$ is the ratio of the field envelope. In order to get an isolated attosecond pulse, the deflection angle difference between subsequent optical cycles should be larger than the harmonic divergence δ,

$$\varphi(t) - \varphi(t \pm T) \geqslant \delta. \tag{2}$$

Moreover, the FWHM of the time-dependent deflection angle should ideally be a single cycle which can be estimated as $\tau_{\text{gating}} = \tau_2\sqrt{2\log_2(2+\xi_0)}$ when $\tau_2 \ll \tau_1$. By Eqs. (1) and (2), the conditions for the field amplitude $\xi_0 \geqslant \delta/(\theta - \delta)$ and the gating pulse duration $\tau_2 \leqslant T_0\sqrt{\frac{2\ln(2)}{\ln\varphi_0 - \ln(\varphi_0-\delta)}}$ must be satisfied.

In our particle-in-a-cell (PIC) simulation, the main pulse intensity was $I_1 = 1 \times 10^{21}$ W/cm^2 with $\tau_1 = 21$ fs and imposing the superposition angle $\theta = 170$ mrad. The harmonic divergence was 17 mrad, which was calculated with a PIC simulation. Thus the gating pulse intensity I_2 with duration $\tau_2 = 2.67$ fs must satisfy the condition $I_2 > 1 \times 10^{19}$ W/cm^2. It is important to note that these duration and intensity requirements apply exclusively to the gating beam. Given that the gating pulse intensity can be significantly lower than that of the main pulse, achieving ultrashort laser pulses is more feasible [28].

For a more rigorous analysis, we performed two-dimensional PIC simulations using SMILEI [29]. The resolution of the spatial grid in the PIC simulations was set to be 256 cells/λ_0, and the size of the simulation box was $20\lambda_0$ and $40\lambda_0$ for the x and y axes, respectively, as shown in Fig. 1. The density and the scale length of the plasma slab were $636n_c$ and $0.05\lambda_0$, respectively. The target was placed slightly away (a half of the Rayleigh range) from the focus so that the incident laser beam is slightly diverging on the plasma surface. With this configuration, the wave-front curvature imposed by the plasma denting will be compensated, reducing the divergence of the generated attosecond pulses. The reflected field is captured at each time step on a probe plane located at a position $28\lambda_0$ away from the target surface. The far-field distribution at an infinite distance is calculated by simply Fourier transforming the electromagnetic field.

In our simulation, we used two p-polarized laser fields, main and gate pulses, that have different intensities. The attosecond pulses are emitted by the main laser pulse whose intensity is $I_1 = 1 \times 10^{21}$ W/cm^2. The main pulse is focused on the plasma surface with an angle of 45°. The size of the focal spot is 2.4 μm. A single-cycle laser pulse is used as a gate pulse. The intensity of the gate pulse is $I_2 = 1.9 \times 10^{19}$ W/cm^2, which is two orders of magnitude weaker. The superposition angle θ between the main and gate pulses is 170 mrad as shown in Fig. 1. The divergence of the attosecond pulses is approximately 17 mrad.

Figure 2 shows the angle-resolved far-field spectrum obtained through PIC calculations. This spectrum is obtained by taking the Fourier transform of the electric field captured by a one-dimensional probe placed $28\lambda_0$ away from the plasma surface. Figures 2(a) and 2(b) show the far field obtained with and without the gating pulse, respectively. The use of the gating pulse gives a rise of an off-axis continuum spectrum [marked with red dashed lines in Fig. 2(b)], clearly showing the effect of the noncollinear gating.

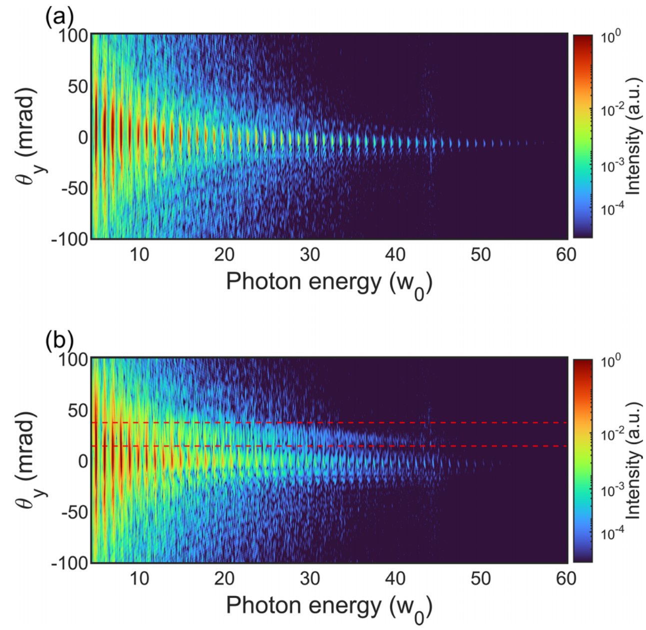

FIG. 2. The angle-resolved far-field spectra obtained from two-dimensional PIC simulations (a) without and (b) with a gating pulse. The main pulse (duration $\tau_1 = 21$ fs, center wavelength $\lambda_0 = 800$ nm, peak intensity $I_1 = 1 \times 10^{21}$ W/cm^2) and the gating pulse ($\tau_2 = 2.67$ fs, $\lambda_0 = 800$ nm, $I_2 = 1.9 \times 10^{19}$ W/cm^2) are used with the superposition angle $\theta = 170$ mrad and the time delay $\Delta t = -8$ fs. The red dashed lines show the range of the quasicontinuum spectrum produced by adding the gating pulse.

The spatiotemporal profiles of the high harmonic emission are analyzed in Fig. 3. The spatiotemporal profile of the attosecond pulse train, generated using the main pulse and the gating pulse, is illustrated in Fig. 3(a). A single isolated attosecond pulse near $t = -3T_0$ has a different propagation angle from the train, which can be simply selected by spatial filtering, ranging from 10 to 45 mrad [the filtering range is marked with red dashed lines in Fig. 3(a)]. The intensity profile obtained by spatial filtering is shown in Fig. 3(b), which clearly demonstrates the generation of an isolated attosecond (as) pulse. The duration of this isolated attosecond pulse is 399 as. For comparison, the attosecond pulse train obtained without the gate pulse and spatial filtering is also shown in Fig. 3(c). These results demonstrate the effectiveness of our approach to obtain an isolated attosecond pulse through relativistic high harmonic generation.

Although it is ideal to use a near-single-cycle pulse, the pulse duration of the gating pulse can be slightly longer if the range of the spatial filtering is properly set. We performed the same simulation with a gating pulse duration of 1.5 optical cycle (4 fs). The temporal profile of the attosecond pulse is shown in Fig. 3(d). Since the use of the longer gating pulse changes the wave front of the adjacent attosecond pulses, the spatial filtering was applied for a narrower range from 25 to 45 mrad. Although the intensity of the attosecond pulse is reduced due to the reduced range, this relaxed condition enables the generation of the isolated attosecond pulse with a slightly longer gating pulse.

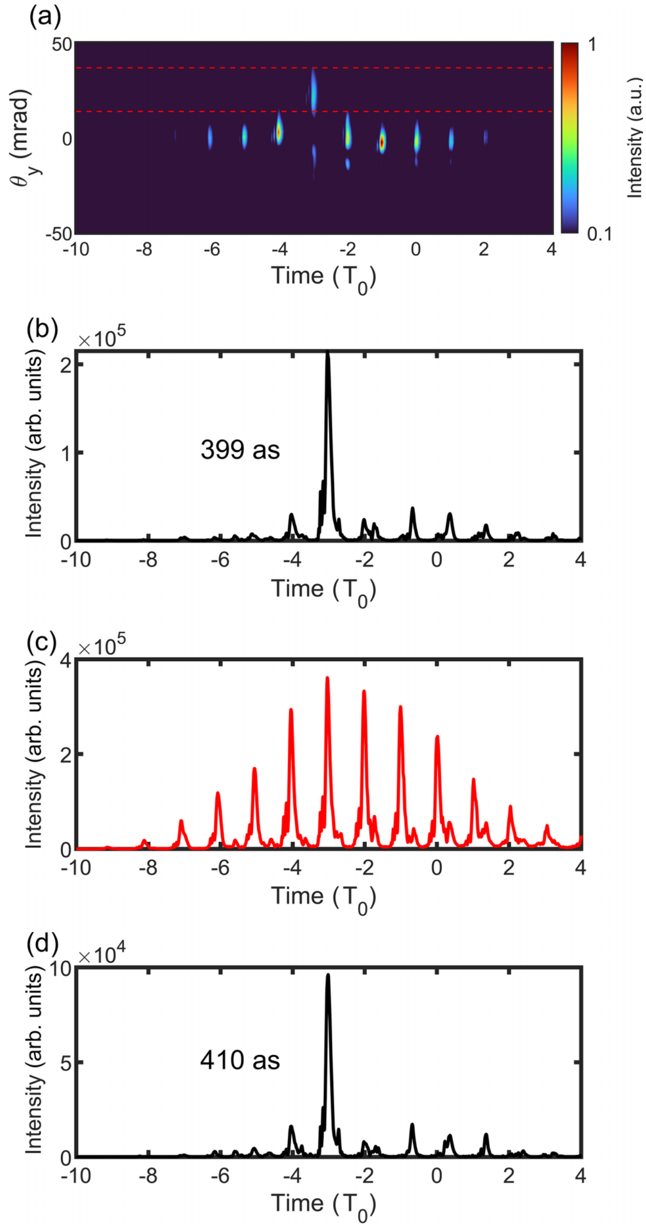

FIG. 3. Two-dimensional PIC simulation result of noncollinear gating of relativistic high harmonic. The same calculation parameters used in Fig. 2 are used. (a) Spatiotemporal profile in the far field. (b) Isolated attosecond pulse selected by spatial filtering for the propagation angle between 10 and 45 mrad in the far field [as indicated by the dotted red line in (a)]. (c) The attosecond pulse train generated without gating pulse. (d) Isolated attosecond pulse obtained using a 1.5-optical-cycle-duration gating pulse, which is selected by spatial filtering for the propagation angle between 25 and 45 mrad in the far field.

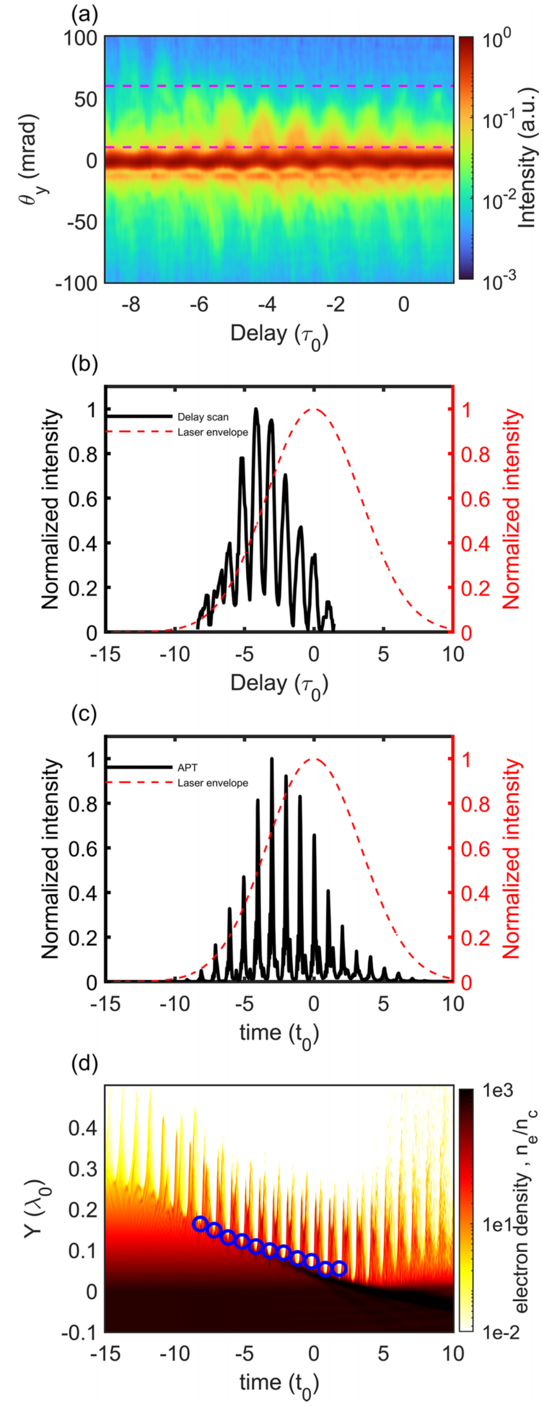

FIG. 4. Probing laser-plasma interaction using noncollinear gating. (a) Spatial profile of the harmonic emission obtained for different time delays from $-8.75T_0$ to $1.44T_0$ at intervals of $0.0625T_0$. The spatial profile of the harmonic emission is obtained by integrating harmonic orders between the 16th and 43rd harmonics. (b) The intensity of the harmonic emission obtained by integrating the propagation angle from 10 to 60 mrad as indicated by the dashed pink lines in (a). (c) The intensity of the attosecond pulse train used in the PIC calculation. (d) Temporal variation of the plasma density profile. The blue dots show the reflection (or emission) position η_{dent} estimated from the chirp of the temporal profile shown in (b).

Our approach also offers an effective way to directly access individual attosecond pulses of an attosecond pulse train. By adjusting the time delay between the main and the gate pulse, we can choose any attosecond pulse from the train. Figure 4 illustrates the effects of varying the time delay of the gate pulse. The intensity of the selected attosecond pulse is obtained for different time delays by spatially filtering the attosecond pulse for the range marked by pink dotted lines in Fig. 4(a). Since the gate pulse deflects a single attosecond pulse consecutively from the train as we change the time delay, the temporal profile of the attosecond pulse train can be visualized as shown in Fig. 4(b). For comparison, the temporal profile of the original attosecond pulses directly obtained from the PIC calculation is shown in Fig. 4(c). These results demonstrate that the temporal profile obtained from spatial filtering represents the temporal profile of the original attosecond pulse. Therefore, noncollinear gating offers a quantitative method for measuring the temporal profile of attosecond pulses.

The temporal profile of the attosecond pulses can also unveil the emission time or the reflection position of the attosecond pulses, which can be changed during the laser-plasma interaction. As depicted in Fig. 4(d), the gradient of the plasma density varies in time due to the radiation pressure of the laser field, which is known as plasma denting effects. We found that the group delay of the attosecond pulse is closely related to the plasma denting effect because the reflection position is varied in time. The group delay τ_k of the kth attosecond pulse can be related to the reflection position η_k as $\tau_{k+1} - \tau_k = T_0 + (2/c)(\eta_{k+1} - \eta_k)\cos\theta_i$. Here, θ_i denotes the incidence angle of the laser pulse. The reflection positions found using this relation are shown with blue circles in Fig. 4(d). These results reveal that the plasma surface is pushed inwards with an average speed of $0.0148c$ due to the radiation pressure, showing good agreement with the gradually varying plasma density. These results confirm that noncollinear gating is useful not only for the generation of an isolated attosecond pulse, but also for probing the laser-plasma interactions.

III. CONCLUSION

In summary, we demonstrated a noncollinear gating technique that can be applied for HHG from relativistic plasma mirrors. The isolation of the attosecond pulse, generated by an intense and long main pulse, is achieved by introducing a weak single-cycle gating pulse superposed with a small angle. The intensity of the gating pulse can be two orders of magnitude lower than that of the main pulse. Thus, our approach can be applied for relativistic HHG in which a high-power main pulse is essentially required.

By separating the isolated attosecond pulse, we could directly analyze the temporal profile of the attosecond pulse train. Adjusting the time delay between the two laser pulses allows us to observe the attosecond pulse train and gain insights into the laser-plasma interaction. Our findings show that the temporal separations of the attosecond pulses vary over time, manifesting the plasma denting effect occurring due to the radiation pressure of the driving laser pulse. This variation helped us reconstruct the reflection position where the attosecond pulses are produced, which is crucial for comprehending the mechanism of relativistic high harmonic generation [30]. Therefore, our method not only offers a practical way to generate isolated attosecond pulses but also facilitates the investigation of laser-plasma interactions with attosecond temporal precision.

Our approach would encounter certain limitations that warrant attention in experimental studies. As the intensity of the main pulse increases, the gating pulse must also be strengthened for the isolation of the attosecond pulse. This is ultimately constrained by the practical challenges of generating intense single-cycle pulses. It is possible to obtain such an ultrashort laser pulse [28] at the intensity level of 10^{19} W/cm^2.

In addition, when using high-power lasers for HHG from a plasma mirror, plasma denting induced by the laser's radiation pressure increases the divergence of the reflected harmonics, which diminishes the effectiveness of the gating pulses. This effect becomes more pronounced with longer plasma scale lengths and smaller laser incidence angles. Nonetheless, as demonstrated in recent work [31], optimizing the focus of the incident pulses or flattening the spatial profile of the beam to minimize plasma mirror curvature can mitigate these effects to some extent. Addressing these challenges will enhance the reliability and applicability of our approach for the isolation of the attosecond pulse.

ACKNOWLEDGMENTS

This work was supported by the Institute for Basic Science Grant No. IBS-R038-D1 and the National Research Foundation of Korea (NRF), Grant No. 2022R1A2C3006025, funded by the Korea government (MIST). Computational works for this research were performed on the IBS Supercomputer Aleph in the IBS Research Solution Center.

DATA AVAILABILITY

Data available on reasonable request from the authors.

[1] D. M. Gold, H. Nathel, P. R. Bolton, W. E. White, and L. D. Van Woerkom, Prepulse suppression using a self-induced ultrashort pulse plasma mirror, Proc. SPIE **1413**, 41 (1991).

[2] H. C. Kapteyn, M. M. Murnane, A. Szoke, and R. W. Falcone, Prepulse energy suppression for high-energy ultrashort pulses using self-induced plasma shuttering, Opt. Lett. **16**, 490 (1991).

[3] M. Ferray, A. L'Huillier, X. F. Li, L. A. Lompre, G. Mainfray, and C. Manus, Multiple-harmonic conversion of 1064 nm radiation in rare gases, J. Phys. B: At. Mol. Opt. Phys. **21**, L31 (1988).

[4] U. Teubner and P. Gibbon, High-order harmonics from laser-irradiated plasma surfaces, Rev. Mod. Phys. **81**, 445 (2009).

[5] T. Baeva, S. Gordienko, and A. Pukhov, Theory of high-order harmonic generation in relativistic laser interaction with over-dense plasma, Phys. Rev. E **74**, 046404 (2006).

[6] D. an der Brügge and A. Pukhov, Enhanced relativistic harmonics by electron nanobunching, Phys. Plasmas **17**, 033110 (2010).

[7] F. Quéré, C. Thaury, P. Monot, S. Dobosz, Ph. Martin, J.-P. Geindre, and P. Audebert, Coherent wake emission of high-order harmonics from overdense plasmas, Phys. Rev. Lett. **96**, 125004 (2006).

[8] G. Sansone, L. Poletto, and M. Nisoli, High-energy attosecond light sources, Nat. Photon. **5**, 655 (2011).

[9] E. Goulielmakis *et al.*, Single-cycle nonlinear optics, Science **320**, 1614 (2008).

[10] R. Kienberger, E. Goulielmakis, M. Uiberacker, A. Baltuska, V. Yakovlev, F. Bammer, A. Scrinzi, T. Westerwalbesloh, U. Kleineberg, and U. Heinzmann, Atomic transient recorder, Nature (London) **427**, 817 (2004).

[11] T. Witting, F. Frank, W. A. Okell, C. A. Arrell, J. P. Marangos, and J. W. G. Tisch, Sub-4-fs laser pulse characterization by spatially resolved spectral shearing interferometry and attosecond streaking, J. Phys. B: At. Mol. Opt. Phys. **45**, 074014 (2012).

[12] I. Thomann, A. Bahabad, X. Liu, R. Trebino, M. M. Murnane, and H. C. Kapteyn, Characterizing isolated attosecond pulses from hollow-core waveguides using multi-cycle driving pulses, Opt. Express **17**, 4611 (2009).

[13] F. Ferrari, F. Calegari, M. Lucchini, C. Vozzi, S. Stagira, G. Sansone, and M. Nisoli, High-energy isolated attosecond pulses generated by above-saturation few-cycle fields, Nat. Photon. **4**, 875 (2010).

[14] P. B. Corkum, N. H. Burnett, and M. Y. Ivanov, Subfemtosecond pulses, Opt. Lett. **19**, 1870 (1994).

[15] I. J. Sola, E. Mével, L. Elouga, E. Constant, V. Strelkov, L. Poletto, P. Villoresi, E. Benedetti, J.-P. Caumes, and S. Stagira, Controlling attosecond electron dynamics by phase-stabilized polarization gating, Nat. Phys. **2**, 319 (2006).

[16] H. Vincenti and F. Quéré, Attosecond lighthouses: How to use spatiotemporally coupled light fields to generate isolated attosecond pulses, Phys. Rev. Lett. **108**, 113904 (2012).

[17] K. T. Kim, C. Zhang, T. Ruchon, J.-F. Hergott, T. Auguste, D. M. Villeneuve, P. B. Corkum, and F. Quéré, Photonic streaking of attosecond pulse trains, Nat. Photon. **7**, 651 (2013).

[18] J. A. Wheeler, A. Borot, S. Monchocé, H. Vincenti, A. Ricci, A. Malvache, R. Lopez-Martens, and F. Quéré, Attosecond lighthouses from plasma mirrors, Nat. Photon. **6**, 829 (2012).

[19] S. Zhong, X. He, Y. Jiang, H. Teng, P. He, Y. Liu, K. Zhao, and Z. Wei, Noncollinear gating for high-flux isolated-attosecond-pulse generation, Phys. Rev. A **93**, 033854 (2016).

[20] F. Krausz and M. Ivanov, Attosecond physics, Rev. Mod. Phys. **81**, 163 (2009).

[21] P. Heissler *et al.*, Few-cycle driven relativistically oscillating plasma mirrors: A source of intense isolated attosecond pulses, Phys. Rev. Lett. **108**, 235003 (2012).

[22] S. G. Rykovanov, M. Geissler, J. Meyer-ter-Vehn, and G. D. Tsakiris, Intense single attosecond pulses from surface harmonics using the polarization gating technique, New J. Phys. **10**, 025025 (2008).

[23] J. P. Kennedy, B. Dromey, and M. Yeung, Isolated ultra-bright attosecond pulses via non-collinear gating, New J. Phys. **24**, 113004 (2022).

[24] M. Yeung *et al.*, Noncollinear polarization gating of attosecond pulse trains in the relativistic regime, Phys. Rev. Lett. **115**, 193903 (2015).

[25] Y. Shou, R. Hu, Z. Gong, J. Yu, J. E. Chen, G. Mourou, X. Yan, and W. Ma, Cascaded generation of isolated sub-10 attosecond half-cycle pulses, New J. Phys. **23**, 053003 (2021).

[26] M. Nisoli, S. D. Silvestri, O. Svelto, R. Szipöcs, K. Ferencz, C. Spielmann, S. Sartania, and F. Krausz, Compression of high-energy laser pulses below 5 fs, Opt. Lett. **22**, 522 (1997).

[27] T. Baeva, S. Gordienko, and A. Pukhov, Relativistic plasma control for single attosecond x-ray burst generation, Phys. Rev. E **74**, 065401(R) (2006).

[28] M. Ouillé *et al.*, Relativistic-intensity near-single-cycle light waveforms at kHz repetition rate, Light Sci. Appl. **9**, 47 (2020).

[29] J. Derouillat *et al.*, SMILEI: A collaborative, open-source, multi-purpose particle-in-cell code for plasma simulation, Comput. Phys. Commun. **222**, 351 (2018).

[30] H. Vincenti, S. Monchocé, S. Kahaly, G. Bonnaud, P. Martin, and F. Quéré, Optical properties of relativistic plasma mirrors, Nat. Commun. **5**, 3403 (2014).

[31] H. Kallala, F. Quéré, and H. Vincenti, Techniques to generate intense isolated attosecond pulses from relativistic plasma mirrors, Phys. Rev. Res. **2**, 043007 (2020).